

## Supplementary Information

# Facile target validation in an animal model with intracellularly expressed monobodies

Ankit Gupta<sup>1,2</sup>, Jing Xu<sup>3</sup>, Shirley Lee<sup>3</sup>, Steven T. Tsai<sup>1</sup>, Bo Zhou<sup>3</sup>, Kohei Kurosawa<sup>1,2</sup>, Michael S. Werner<sup>4</sup>, Akiko Koide<sup>1,2,5</sup>, Alexander J. Ruthenburg<sup>4</sup>, Yali Dou<sup>3</sup> and Shohei Koide<sup>1,2,6</sup>

<sup>1</sup>Perlmutter Cancer Center, New York University Langone Medical Center, New York, USA.

<sup>2</sup>Department of Biochemistry and Molecular Biology, The University of Chicago, Chicago, Illinois, USA

<sup>3</sup>Department of Pathology, University of Michigan, Ann Arbor, Michigan, USA

<sup>4</sup>Department of Molecular Genetics and Cell Biology, The University of Chicago, Chicago, Illinois, USA

<sup>5</sup>Department of Medicine, New York University School of Medicine, New York, USA.

<sup>6</sup>Department of Biochemistry and Molecular Pharmacology, New York University School of Medicine, New York, USA.

Correspondence should be addressed to S.K. ([skoide@uchicago.edu](mailto:skoide@uchicago.edu)) or [yvalid@med.umich.edu](mailto:yvalid@med.umich.edu)

### **Table of Contents**

Supplementary Tables 1 and 2.

Supplementary Figures 1-11.

Supplementary Dataset. Mass spectrometry analyses of proteins captured by Mb(S4) or Mb(S4mut) from the whole cell lysate or nuclear extract of HEK293T cells (separate Microsoft Excel file)

**Supplementary Table 1.** Data collection and refinement statistics (molecular replacement)

---

<b>Data collection</b>	
Space group	C 1 2 1
Cell dimensions	
<i>a</i> , <i>b</i> , <i>c</i> (Å)	79.08, 48.27, 99.83
$\alpha$ , $\beta$ , $\gamma$ (°)	90, 107.8, 90
Resolution (Å)	47.5-2.69 (2.79-2.69)*
<i>R</i> <sub>pim</sub>	0.049 (0.203)
<i>I</i> / $\sigma$ <i>I</i>	20.9 (4.0)
Completeness (%)	99.72 (97.44)
Redundancy	6.5 (4.6)
<b>Refinement</b>	
Resolution (Å)	47.5-2.69 (2.79-2.69)
No. of reflections	10148 (953)
<i>R</i> <sub>work</sub> / <i>R</i> <sub>free</sub>	0.2156/0.2484
No. atoms	3152
Protein	3083
Ligand/ion	0
Water	69
<i>B</i> -factors	36.20
Protein	36.20
Ligand/ion	0
Water	35.00
R.m.s deviations	
Bond lengths (Å)	0.002
Bond angles (°)	0.69

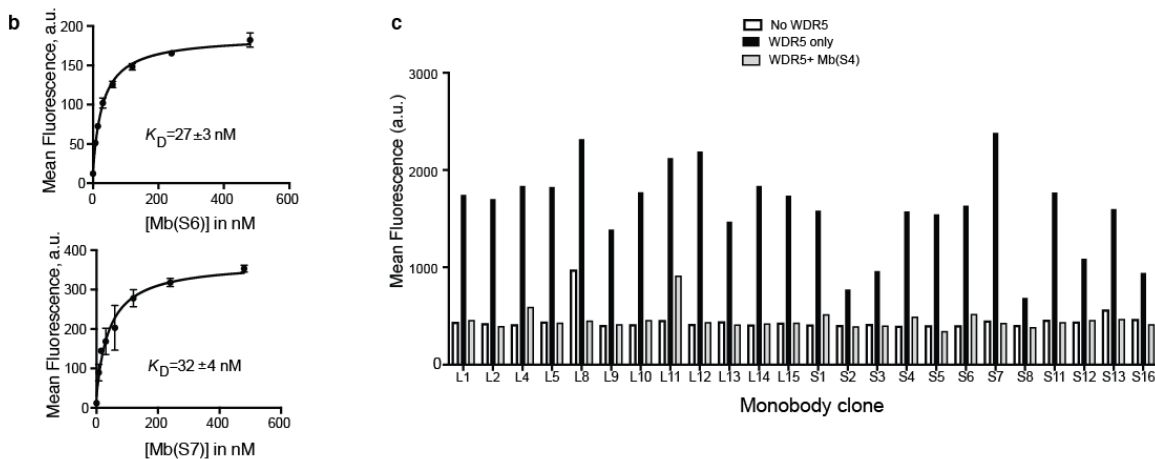
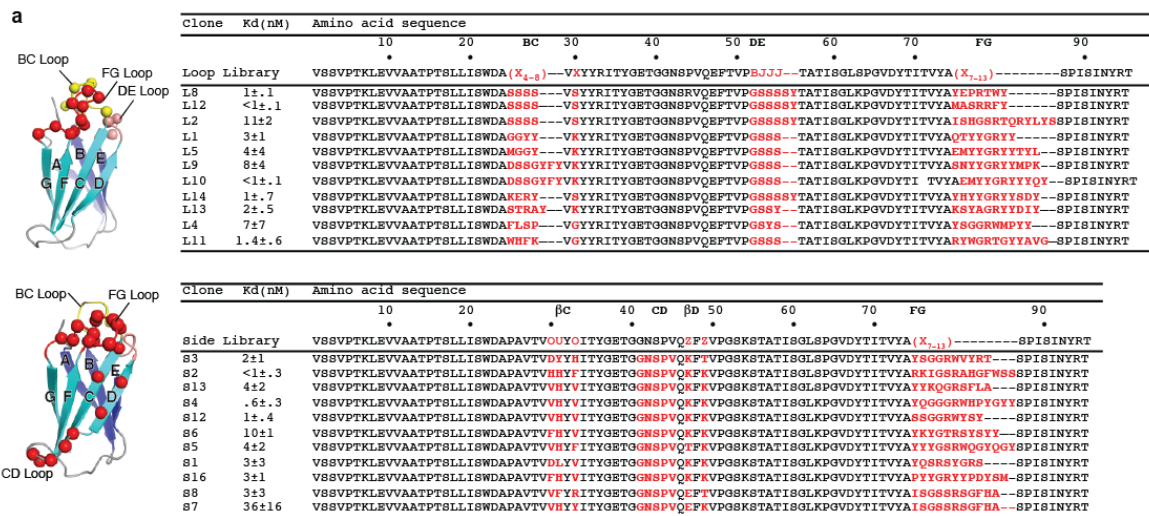
---

Number of crystals used: 1. \*Highest-resolution shell is shown in parentheses.

**Supplementary Table 2. Comparison of WDR5–MLL1 Win and WDR5–Mb(S4) interfaces**

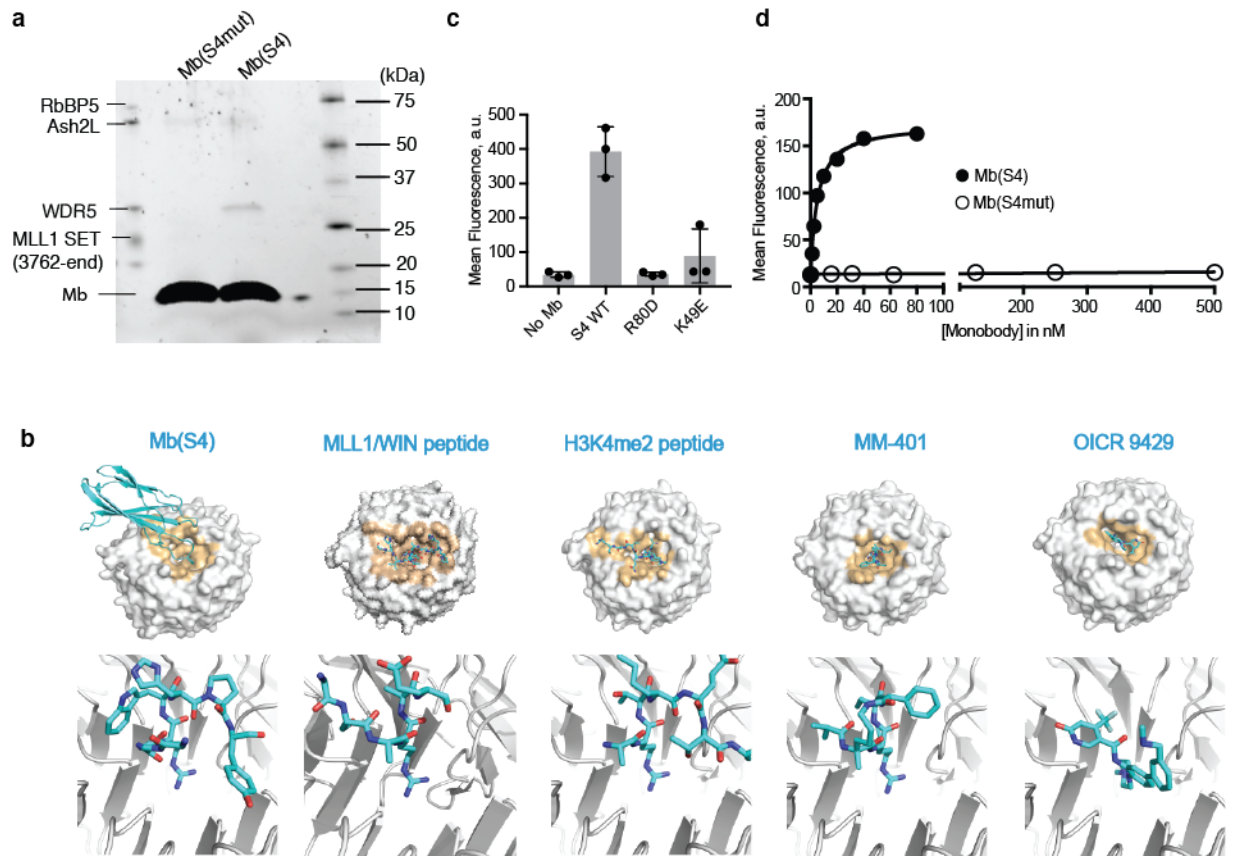
Ligand	MLL1 Win <sup>1</sup>	Mb(S4)
interface (Å <sup>2</sup> )	686.5	698.7
Number of WDR5 residues <sup>2</sup>	26	26
<i>WDR5 residue in interface</i>		
Residue	BSA <sup>3</sup> (Å <sup>2</sup> )	
K46	42.0	–
A47	12.7	14.1
S49	17.8	19.3
A65	37.8	30.8
K67	6.2	–
L88	34.8	–
G89	15.8	10.8
I90	3.5	3.6
S91	25.8	27.3
D107	37.3	35.5
N130	26.5	21.0
Y131	–	41.6
F133	41.9	38.4
C134	3.0	2.5
F149	37.0	67.0
E151	–	22.0
S171	–	9.1
D172	1.2	24.4
P173	17.2	24.9
S175	5.2	5.1
Y191	43.6	39.7
F219	3.8	3.6
P234	1.0	–
K259	40.5	37.9
Y260	50.7	51.5
C261	12.2	12.3
F263	15.8	16.4
I305	13.9	15.2
L321	19.6	15.9
E322	0.3	4.4
<i>Mb(S4) residue in interface</i>		
Residue	BSA (Å <sup>2</sup> )	
V30	50.9	
H31	18.9	
K49	63.7	
Q76	3.8	
G77	12.7	
G78	56.0	
G79	25.2	
R80	232.4	
W81	162.6	
P83	73.6	
Y84	99.8	

The interface properties were analyzed using PDBe PISA server (version 1.52; [http://www.ebi.ac.uk/msd-srv/prot\\_int/cgi-bin/piserver](http://www.ebi.ac.uk/msd-srv/prot_int/cgi-bin/piserver)). <sup>1</sup>Chains A and D in PDB ID 4ESG (Dharmarajan, V., Lee, J.H., Patel, A., Skalnik, D.G. & Cosgrove, M.S. Structural basis for WDR5 interaction (Win) motif recognition in human SET1 family histone methyltransferases. *J Biol Chem* **287**, 27275-89 (2012)). <sup>2</sup>Defined here as a residue with buried surface area no less than 1.0 Å<sup>2</sup>. <sup>3</sup>Buried surface area.



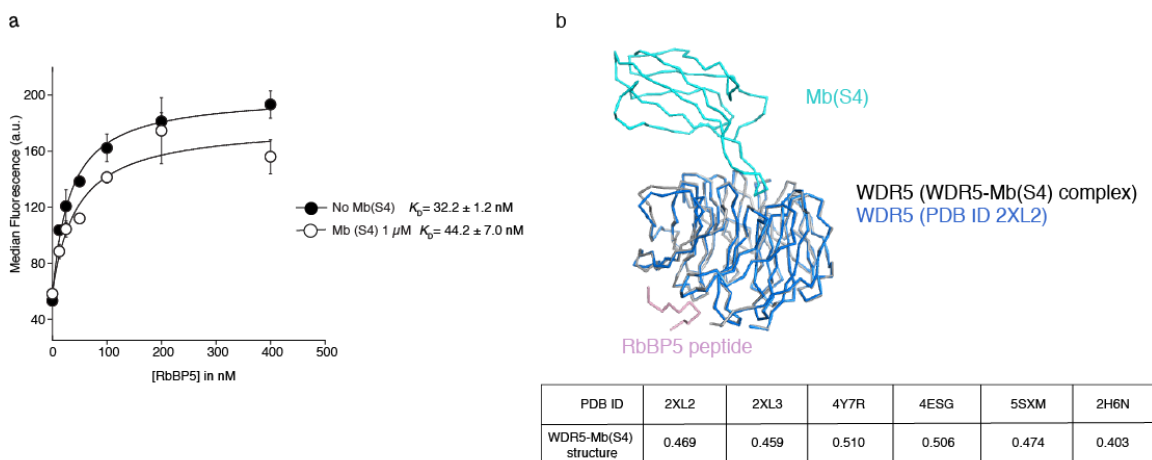
**Supplementary Figure 1. Monobodies binding to WDR5. (a)** The amino acid sequences of the monobodies and their  $K_D$  values measured in yeast display format. The designs of the two libraries from which these monobodies were derived are also shown in the table and also as cartoons. In the cartoons, the  $\beta$ -strands and loops are labeled and the diversified residues are marked as red spheres. In the library designs, 'X' denotes a mixture of 30% Tyr, 15% Ser, 10% Gly, 5% Phe, 5% Trp, and 2.5% each of all the other amino acids except for Cys, 'B', a mixture of Gly, Ser and Tyr, 'J', a mixture of Ser and Tyr, 'O', a mixture of Asn, Asp, His, Ile, Leu, Phe, Tyr, and Val, 'U', a mixture of His, Leu, Phe and Tyr, 'Z', a mixture of Ala, Glu, Lys and Thr<sup>1</sup>. A hyphen indicates a deletion. Residues marked in red correspond to the diversified regions in the monobody scaffold, also shown as spheres in the molecular graphics. **(b)** Titration curves for binding of Mb(S6) and Mb(S7) to WDR5 in a bead based binding assay. Data are presented as mean  $\pm$  s.d. from  $n=3$  independent experiments. The curves show the best fit to the 1:1 binding model. **(c)** Competitive binding assay of monobody clones. Monobodies displayed on the yeast surface were tested for binding to 10 nM WDR5 in the absence and presence of 50 nM purified Mb(S4) protein. Binding of all the clones was competed by purified Mb(S4) protein (compare "WDR5 only" (black bars) with "WDR5+Mb(S4)" (grey bars)), suggesting that all monobodies bind to overlapping epitopes.

1. Koide, A., Wojcik, J., Gilbreth, R.N., Hoey, R.J. & Koide, S. Teaching an old scaffold new tricks: monobodies constructed using alternative surfaces of the FN3 scaffold. *J Mol Biol* **415**, 393-405 (2012)



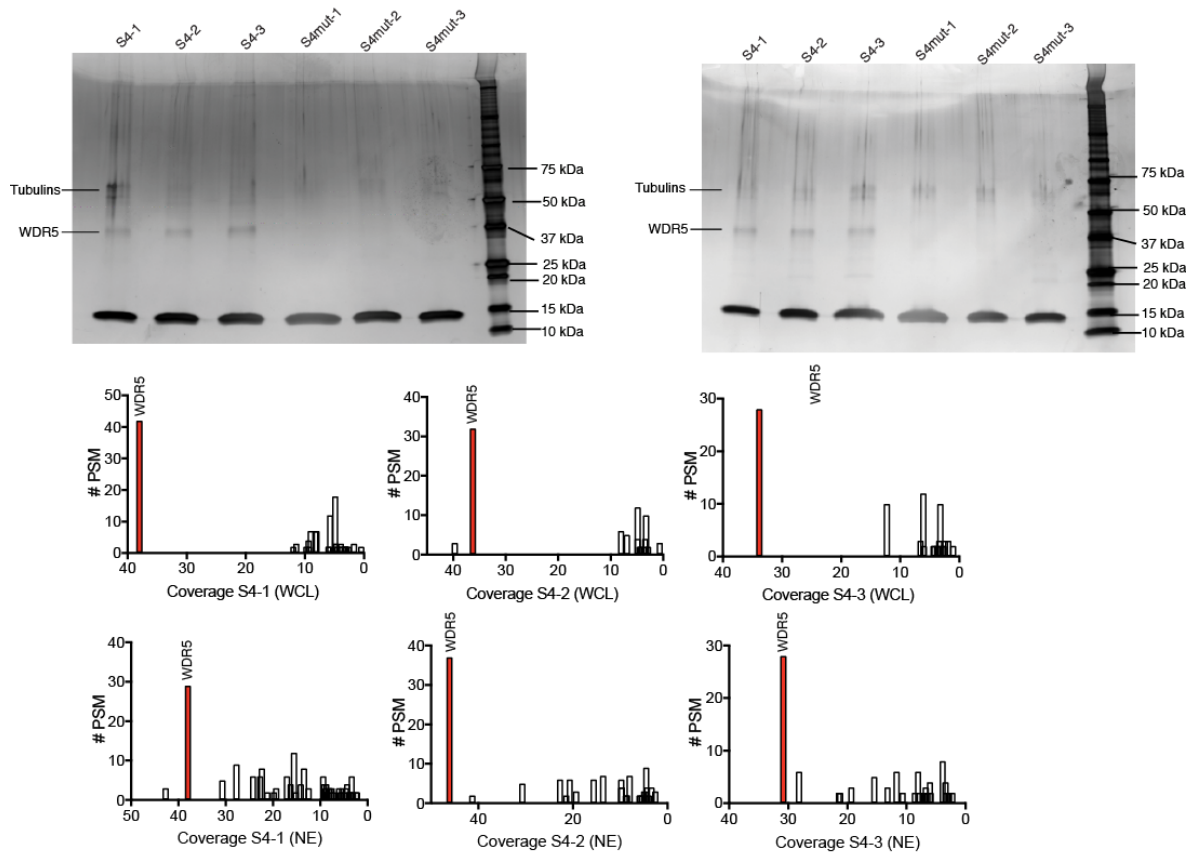
**Supplementary Figure 2. Biochemical functions and structure of Mb(S4)** (a) Capture of WDR5 and additional components from *in vitro* reconstituted MLL1 complex with Mb(S4). Lane 1, input MLL1 complex; Lane 2, material captured with Mb(S4mut); Lane 3, material captured with Mb(S4); Lane 4, Precision Plus Protein™ Unstained Standard Marker. The proteins were separated using SDS-PAGE and visualized with Krypton staining. The data shown are from  $n=1$  experiment. (b) The MLL1 binding pocket of WDR5. Comparison of the crystal structures of WDR5 in complex with different interaction partners. WDR5 is shown in surface presentation with the interacting residues in brown (top). Interacting regions of Mb(S4), MLL1 (PDB ID 4ESG)<sup>1</sup>, H3K4me2 peptide (PDB ID 2H6N)<sup>2</sup>, MM-401 (PDB ID 4GM9)<sup>3</sup> and OICR 9429 (PDB ID 4QL1)<sup>4</sup> with WDR5 are shown (bottom). (c) Binding of Mb(S4) and its mutants (32 nM) to WDR5 immobilized on magnetic beads as tested using the bead binding assay. Data are presented as mean  $\pm$  s.d. from  $n=3$  independent experiments. (d) Binding of purified Mb(S4) and Mb(S4mut), i.e. R80D/W81A, to biotinylated WDR5 immobilized on streptavidin M280 beads. Data are representative of  $n=3$  independent experiments.

1. Dharmarajan, V., Lee, J.H., Patel, A., Skalnik, D.G. & Cosgrove, M.S. Structural basis for WDR5 interaction (Win) motif recognition in human SET1 family histone methyltransferases. *J Biol Chem* **287**, 27275-89 (2012).
2. Ruthenburg, A.J. et al. Histone H3 recognition and presentation by the WDR5 module of the MLL1 complex. *Nat Struct Mol Biol* **13**, 704-12 (2006).
3. Cao, F. et al. Targeting MLL1 H3K4 methyltransferase activity in mixed-lineage leukemia. *Mol Cell* **53**, 247-61 (2014).
4. Grebien, F. et al. Pharmacological targeting of the Wdr5-MLL interaction in C/EBPalpha N-terminal leukemia. *Nat Chem Biol* **11**, 571-8 (2015).

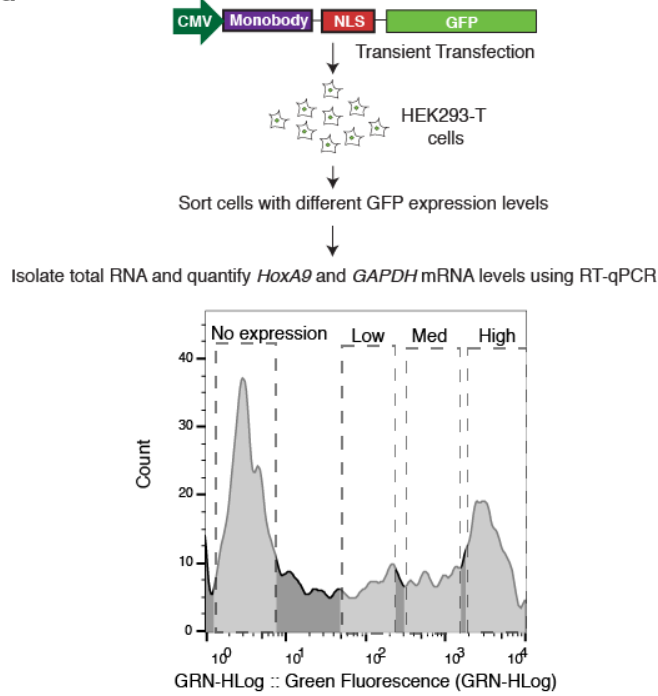
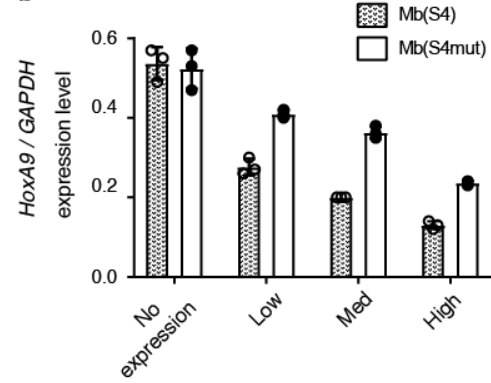


**Supplementary Figure 3. Mb(S4) does not affect WDR5-RbBP5 interaction.** (a) Binding titration curves for RbBP5 to immobilized WDR5 in the absence and presence of 1  $\mu$ M Mb(S4), as measured using a bead based binding assay, showing little effect of Mb(S4) on the WDR5-RbBP5 interaction. Data are presented as mean  $\pm$  s.d. from  $n=3$  independent experiments. The curves show the best fit to the 1:1 binding model. (b) Overlay of the crystal structure of the WDR5-Mb(S4) complex with the WDR5-RbBP5 structure (PDB ID 2XL2) showing very similar WDR5 conformations. Also shown are the backbone RMSDs between the WDR5-Mb(S4) structure with other published structures: WDR5-RbBP5 peptide (PDB ID 2XL2)<sup>1</sup>, WDR5-RbBP5 peptide-H3.1 peptide complex (PDB ID 2XL3)<sup>1</sup>, WDR5-MycIIIb peptide (PDB ID 4Y7R)<sup>2</sup>, WDR5-MLL1 Win peptide (PDB ID 4ESG)<sup>3</sup>, WDR5-MLL Win motif peptidomimetic (PDB ID 5SXM)<sup>4</sup> and WDR5-H3K4me2 peptide (PDB ID 2H6N)<sup>5</sup>.

1. Odho, Z., Southall, S.M. & Wilson, J.R. Characterization of a novel WDR5-binding site that recruits RbBP5 through a conserved motif to enhance methylation of histone H3 lysine 4 by mixed lineage leukemia protein-1. *J Biol Chem* **285**, 32967-76 (2010).
2. Thomas, L.R. et al. Interaction with WDR5 promotes target gene recognition and tumorigenesis by MYC. *Mol Cell* **58**, 440-52 (2015).
3. Dharmarajan, V., Lee, J.H., Patel, A., Skalnik, D.G. & Cosgrove, M.S. Structural basis for WDR5 interaction (Win) motif recognition in human SET1 family histone methyltransferases. *J Biol Chem* **287**, 27275-89 (2012).
4. Alicea-Velazquez, N.L. et al. Targeted Disruption of the Interaction between WD-40 Repeat Protein 5 (WDR5) and Mixed Lineage Leukemia (MLL)/SET1 Family Proteins Specifically Inhibits MLL1 and SETd1A Methyltransferase Complexes. *J Biol Chem* **291**, 22357-22372 (2016).
5. Ruthenburg, A.J. et al. Histone H3 recognition and presentation by the WDR5 module of the MLL1 complex. *Nat Struct Mol Biol* **13**, 704-12 (2006).

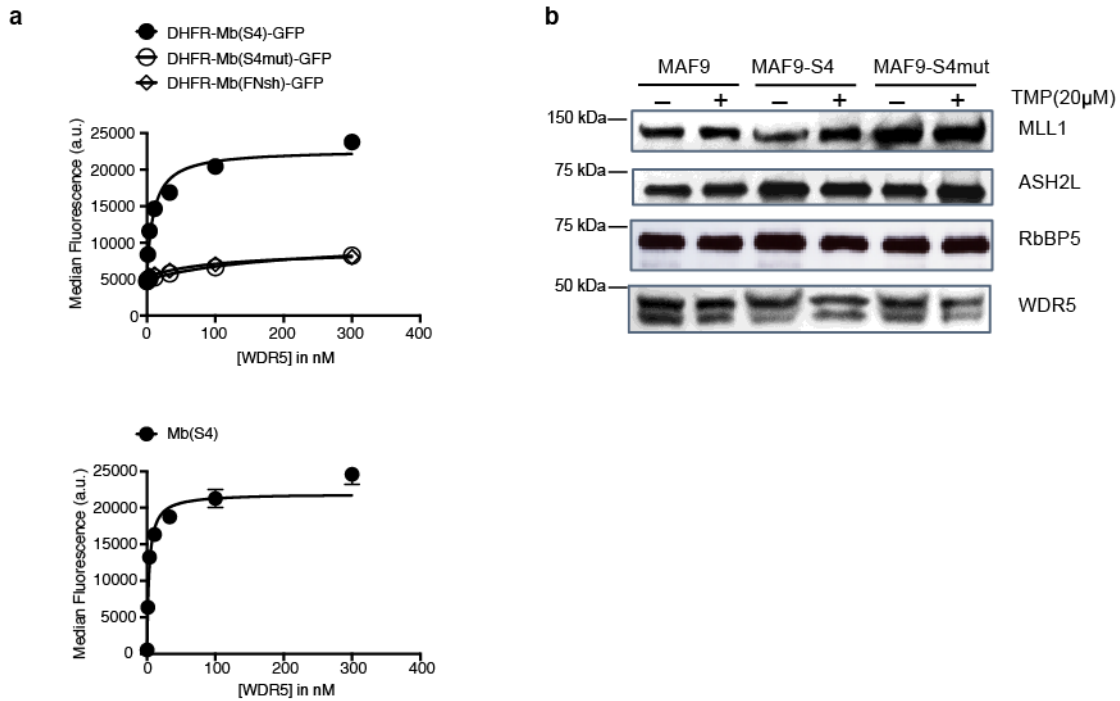


**Supplementary Figure 4. Specificity assessment of Mb(S4) by immunoprecipitation-like experiments.** Capture of proteins from HEK293-T whole cell lysates (left) and nuclear extracts (right) using Mb(S4) and Mb(S4mut) as the capture reagents. The samples captured with the monoclonal antibodies were separated on SDS-PAGE and visualized using silver staining. Lanes S4-1, S4-2 and S4-3 (or S4mut-1, S4mut-2 and S4mut-3) in the two gels correspond to elution from immunoprecipitation-like experiments in triplicates using Mb(S4) (or Mb(S4mut)). Position of tubulins and WDR5 separated on SDS-PAGE based on molecular weights is shown. On the bottom, the plots of peptide spectral matches *versus* sequence coverage for immunoprecipitation experiments using Mb(S4) as analyzed by mass spectrometry with whole cell lysates (WCL) and nuclear extracts (NE) prepared from HEK293-T cells. Data for WDR5 are highlighted in red. Data from  $n=3$  independent experiments are shown.

**a****b**

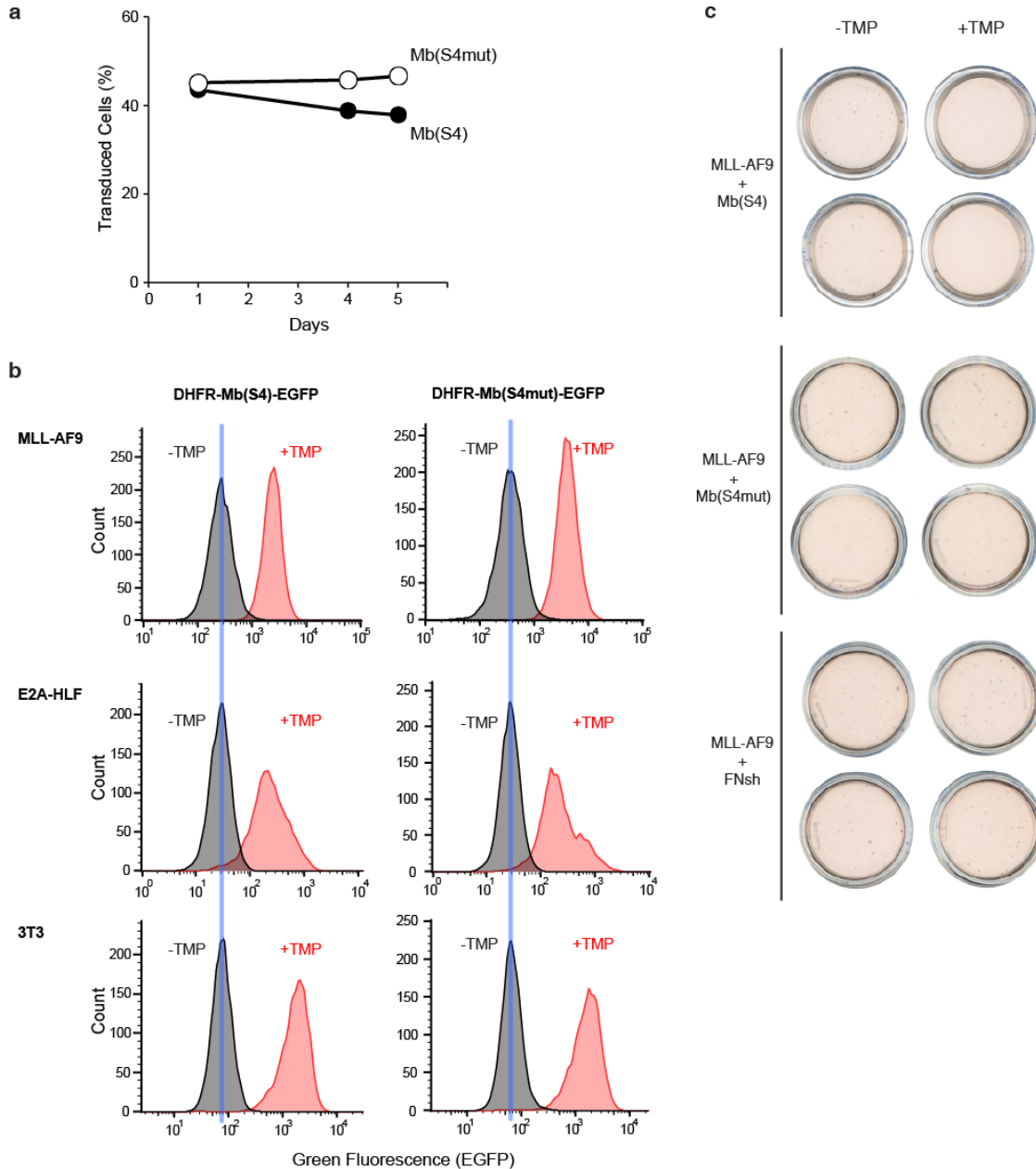
**Supplementary Figure 5. Effects of Mb(S4) expression on the *HoxA9* expression level in HEK293-T cells.** (a) Scheme for sorting of transfected HEK293-T cells with different expression levels of monobody using GFP as marker. (b) RT-qPCR for *HOXA9* in transiently transfected HEK293-T cells with different expression levels of Mb(S4) or Mb(S4mut). The expression level was normalized against that of *GAPDH*. Data are presented as mean  $\pm$  s.d. from  $n=3$  independent experiments.



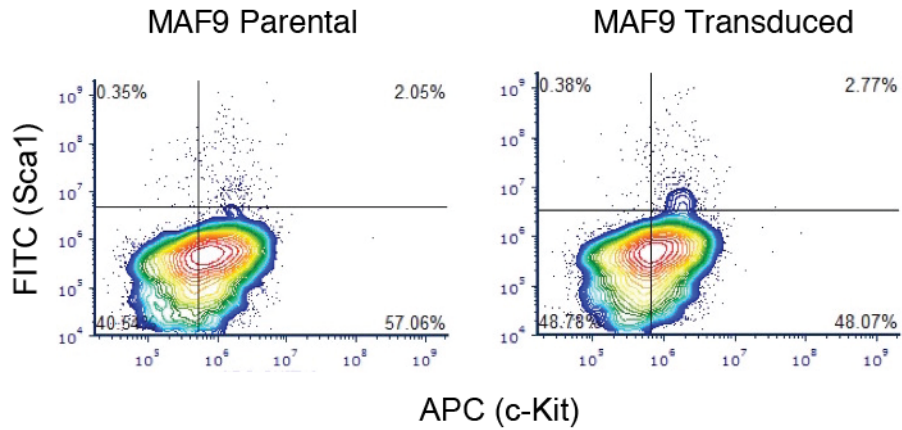


**Supplementary Figure 6.** (a) Minimal effect of fusing Mb(S4) to DHFR and EGFP on Mb(S4) function. DHFR-Mb(S4)-EGFP, DHFR-Mb(S4mut)-EGFP and DHFR-Mb(FNsh)-EGFP (nonbinding, negative control monobody) expressed in HEK293T cells were captured by GFP-binding monobody<sup>1</sup> conjugated to Dynabeads M280 and binding titration of purified WDR5 protein was performed using the bead binding assay. The lower panel shows a reference experiment in which purified, nonfusion Mb(S4) was directly immobilized onto Dynabeads M280. Data are presented as mean  $\pm$  s.d. from  $n=3$  independent experiments. The nearly identical titration curves for DHFR-Mb(S4)-EGFP and nonfusion Mb(S4) indicate that fusion of Mb(S4) to DHFR and EGFP did not significantly influence its function. (b) Western blotting showing that there were minimal effects of monobody expression on protein levels of WDR5 and other MLL core components. Western blotting of MLL-AF9 cells transduced with the indicated monobodies with and without TMP addition for the indicated proteins. Antibodies for western blot are indicated on right. Data are representative of  $n=3$  independent experiments. Uncropped images are provided in Supplementary Fig. 11.

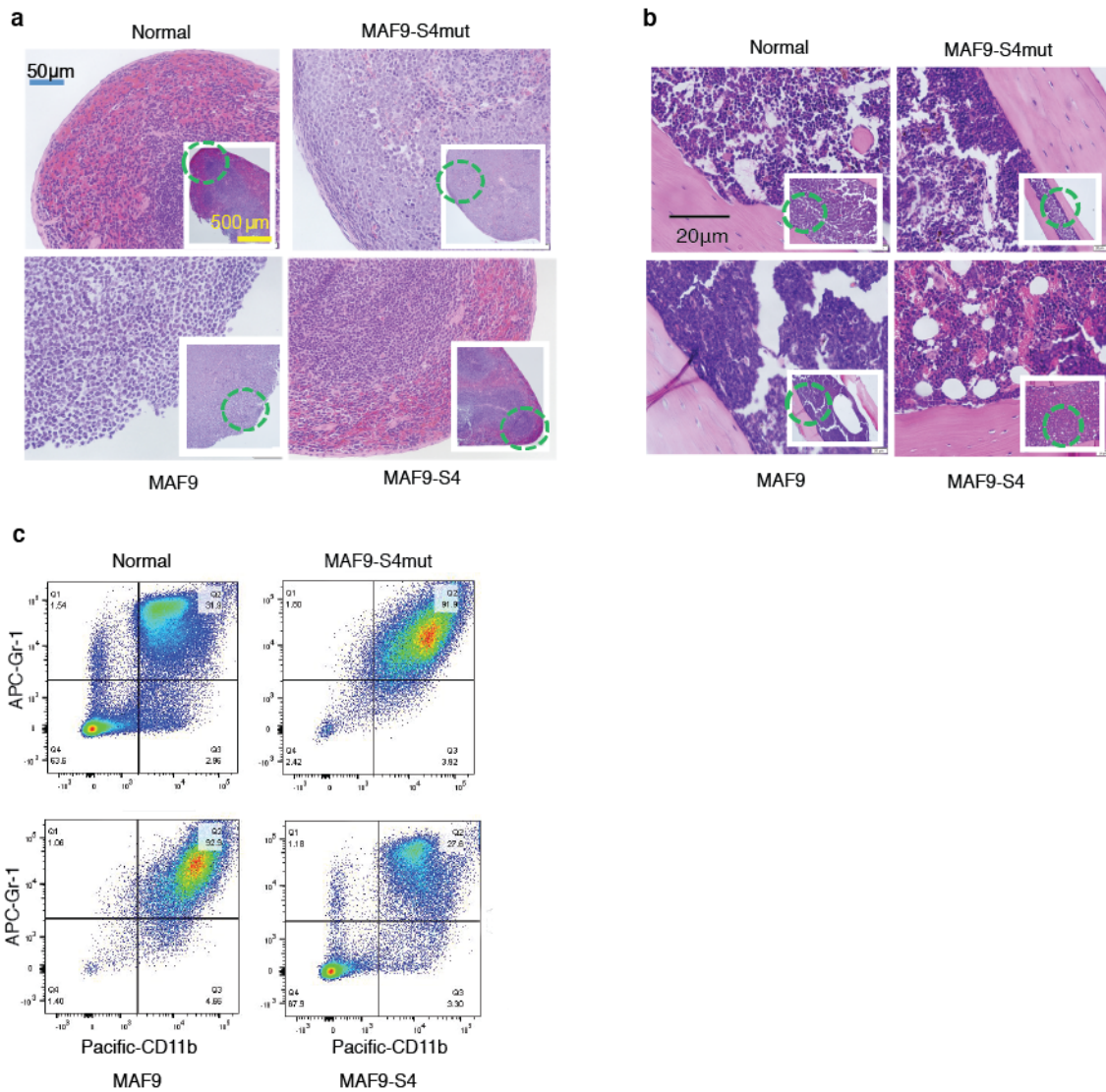
1. Koide, A., Wojcik, J., Gilbreth, R.N., Hoey, R.J. & Koide, S. Teaching an old scaffold new tricks: monobodies constructed using alternative surfaces of the FN3 scaffold. *J Mol Biol* **415**, 393-405 (2012)



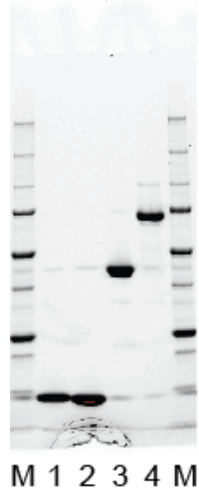
**Supplementary Figure 7.** Cellular effects of Mb(S4) expression. **(a)** Cell proliferation assay of NIH-3T3 cells transduced with Mb(S4) or Mb(S4mut) with induction of the monobodies with TMP. Data are presented as mean  $\pm$  s.d. from  $n=4$  independent cell cultures. Error bars are within the size of the symbols. **(b)** Expression levels of DHFR-Mb(S4)-EGFP and DHFR-Mb(S4mut)-EGFP in MAF9, E2A-HLF and 3T3 cell lines, as measured using EGFP fluorescence. The measurements were taken 42 hours after TMP addition using identical settings for the flow cytometer. For comparison, the profiles for different cell lines are aligned using the emission profiles of the no induction (no TMP) samples, as guided with the vertical blue lines. These experiments were repeated twice with similar results. **(c)** Clonogenic assays using bone marrow progenitor cells transduced with MLL-AF9 and the indicated monobody, treated with or without TMP. Related to Figure 2d. These experiments were repeated twice with similar results.



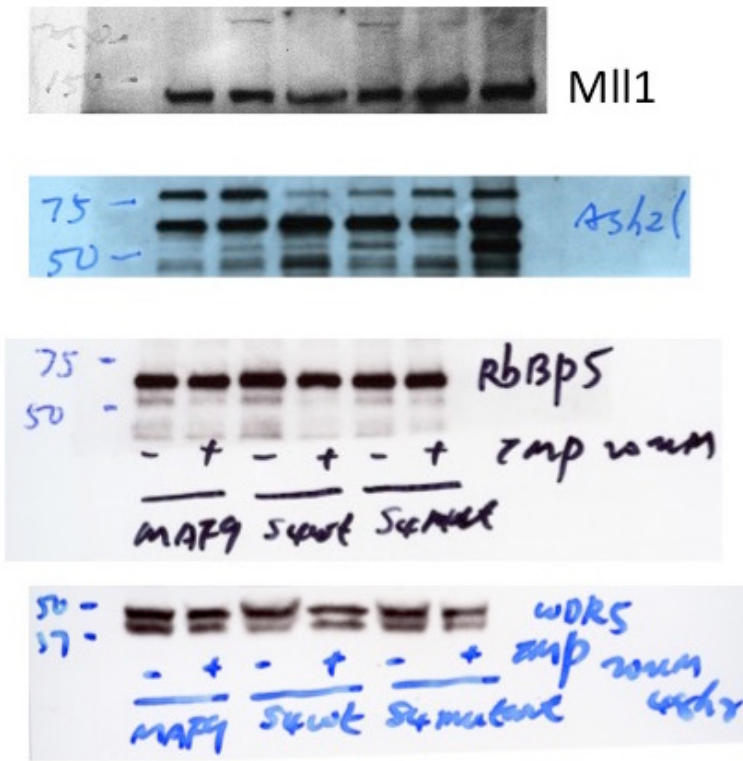
**Supplementary Figure 8.** Viral transduction and cell culture under selection conditions reduced the fractions of leukemia stem cells ( $\text{Lin}^-$ ,  $\text{c-Kit}^{\text{high}}$  and  $\text{Sca1}^{\text{low}}$ ; right bottom quadrant) in MAF9 cells. MAF9 cells were transduced with an empty pMSCV vector and cultured in the presence of 10  $\mu\text{g/ml}$  Blasticidin for seven days. The parental and transduced cells were analyzed using flow cytometry. The bottom right quadrant represents the leukemia stem cell population. The percentage value for each quadrant is shown. Data are representative of  $n=3$  independent experiments. These control experiments were performed on a different stock of MAF9 cells from those used in the experiments shown in Figure 4a.



**Supplementary Figure 9.** Characterization of tissue samples from mice transplanted with MLL-AF9 cells expressing Mb(S4) or Mb(S4mut). (a) Histological sections of spleen from each transplanted mice group, as well as normal, non-transplanted mice as a control. The green circle shows the enlarged area. (b) Histological sections of leg bone from each transplanted mice group, non-transplanted mice as normal control. The green circles in the insets show the enlarged area. (c) Flow cytometry analysis of the myeloid population ( $CD11b^+$  and  $Gr-1^+$ ) in bone marrows 40 days post-transplantation as indicated. The data in a-c are representative of  $n=3$  independent experiments.



**Supplementary Figure 10.** SDS-PAGE of purified proteins used in this work. Approximately 2  $\mu$ g each of Mb(WDR5\_S4) (lane 1), Mb(WDR5\_S4mut) (lane 2), WDR5 (lane 3) and RbBP5 (lane 4) samples were separated on a Mini-PROTEAN TSX stain-free precast gel and visualized with direct staining using a ChemDoc instrument (Bio-Rad). Data are representative of  $n=3$  independent purification runs.



**Supplementary Figure 11.** Full blots for Supplementary Figure 6b.